

Synthesis and characterization of $\text{LiMg}_y\text{Mn}_{2-y}\text{O}_4$ cathode materials by a modified Pechini process for lithium batteries

A SUBRAMANIA*, N ANGAYARKANNI, A R SATHIYA PRIYA,
R GANGADHARAN and T VASUDEVAN

Department of Industrial Chemistry, Alagappa University, Karaikudi 630 003, India

MS received 15 December 2004; revised 6 September 2005

Abstract. Cubic spinels of composition, $\text{LiMg}_y\text{Mn}_{2-y}\text{O}_4$, with $y = 0.0, 0.05, 0.1, 0.15$ and 0.2 , were synthesized by a modified Pechini process using polyethylene glycol and citric acid. The phase formation and/or crystallization of the precursors were studied by thermal analysis. Products were characterized by X-ray diffraction and SEM analysis. Coin cells were fabricated with lithium as the anode and $\text{LiMg}_y\text{Mn}_{2-y}\text{O}_4$ as the cathode in an electrolyte of 1 M LiPF_6 in a 1 : 1 (v/v) mixture of EC and DEC. The charge–discharge studies were performed and the results were compared with materials prepared by a solid state thermal method.

Keywords. Lithium batteries; cathode material; modified Pechini process; cubic spinel materials.

1. Introduction

Among the various insertion compounds used in lithium batteries, LiMn_2O_4 spinel is attractive as a positive electrode material due to its low cost and less toxic nature (Ozhuku *et al* 1990; Guyomard and Tarason 1994). However, LiMn_2O_4 suffers from capacity fade, which limits its cyclability. The capacity fading is due to Jahn–Teller distortion effect (Gummow *et al* 1994) and lattice instability of pure spinel compounds at higher oxidation levels (Yamada 1996). But doped spinels have no such distortion effect. Hence capacity fading is independent of temperature. In order to overcome these problems, substitution of some of the manganese with additional lithium ($\text{Li}_{1+x}\text{Mn}_{2-x}\text{O}_4$) or with several cations ($\text{LiM}_y\text{Mn}_{2-y}\text{O}_4$, where $M = \text{Ni}, \text{Co}, \text{Cr}$ and Al) (Morita *et al* 2001; Lee *et al* 2004) has been widely explored. The electrochemical behaviour of these materials also depends upon the method of synthesis (Gummow *et al* 1994). In recent years, several low temperature techniques such as sol–gel (Hwang *et al* 2001), combustion (Kovacheva *et al* 2002), precipitation (Shaju *et al* 2002) and emulsion drying (Myung *et al* 2000) have also been used for the synthesis of LiMn_2O_4 spinels. Although these methods offer a greater degree of homogeneity, they require careful manipulation which may increase the cost of production and it may also require high temperature heating (above 800°C) for 10–12 h to get the final product.

Very recently, Pechini process (U.S. Pat. 1967) has been used for the synthesis of LiMn_2O_4 because it eliminates some drawbacks inherent in the other low temperature

processes and also gives high purity products with controlled stoichiometries. Other low temperature processes are not always effective at maintaining a homogeneous reactant distribution during heating; the result is that undesirable phase can form at the beginning of calcinations (Bach *et al* 1990; Barboux *et al* 1991). But in Pechini process a 1 : 4 molar ratio of citric acid and ethylene glycol is used and several steps are involved to get the polymeric precursor. All these steps are tedious and care must be taken in every step including in the removal of any excess ethylene glycol by heating to about 180°C under reduced pressure. As ethylene glycol is eliminated, polyesterification occurs (Liu *et al* 1996). In order to eliminate the above drawbacks of the Pechini process, in the present investigation, a modified Pechini process is introduced in which both citric acid and PEG are directly used in the reaction process.

Hence in the present study, we have shown the possibility of synthesizing substituted LiMn_2O_4 by a modified Pechini process. The electrochemical behaviour of cathode materials during charging and discharging were also investigated. These results were compared with materials prepared by a solid-state thermal method.

2. Experimental

2.1 Synthesis

Nano-crystalline cubic spinel, $\text{LiMg}_y\text{Mn}_{2-y}\text{O}_4$ ($y = 0.10, 0.15, 0.20, 0.25$) powders, were prepared by a modified Pechini process. AnalaR grade LiNO_3 , $\text{Mg}(\text{NO}_3)_2$ and $\text{Mn}(\text{CH}_3\text{COO})_2$ were used as the starting materials. In this method, stoichiometric amount of LiNO_3 , $\text{Mg}(\text{NO}_3)_2$ and

*Author for correspondence (a_subramania@rediffmail.com)

$\text{Mn}(\text{CH}_3\text{COO})_2$ were taken and made into a homogeneous solution with distilled water. In the above solution, required quantity of citric acid and polyethylene glycol were added and then the solution was heated to 100°C to make it viscous. Interestingly polyethylene glycol acts as a dispersing agent as well as secondary fuel.

According to a concept developed in propellant chemistry (Jain *et al* 1981), the oxidizing valency (O) of LiNO_3 was -5 , $\text{Mg}(\text{NO}_3)_2$, -10 and $\text{Mn}(\text{CH}_3\text{COO})_2$, $+16$ and the reducing valency (F) of citric acid was $+18$. The amount of citric acid required was calculated for $\text{LiMg}_{0.10}\text{Mn}_{1.90}\text{O}_4$ system by using this concept to get

$$1 \times (-5) + (-10 \times 1 \times 0.10) + (16 \times 1 \times 1.90) + 18n = 0, n = 1.35 \text{ M.}$$

Therefore, the required amount of citric acid was 1.35 M. But the amount of PEG optimized empirically was equivalent to the amount of citric acid taken. The same procedure was followed for other ratios such as 0.15, 0.20 and 0.25.

The viscous solution so obtained was further heated to 140°C for 3 h for esterification reaction. This precursor was then pyrolysed at 340°C for 3 h in air. In this way cubic spinel $\text{LiMg}_x\text{Mn}_{2-x}\text{O}_4$ powder was obtained. The resultant products were collected and subjected to both physical characterization and electrochemical studies.

2.2 Physical characteristics

X-ray diffraction measurements were made from JEOL (JDX 8030) X-ray diffractometer using nickel filtered Cu-K α radiation to identify the crystalline phase of the synthesized materials. The thermal decomposition behaviour of the precursor sample, $\text{LiMg}_{0.20}\text{Mn}_{1.80}\text{O}_4$, was made using a simultaneous TG/DTA thermal analyser (STA-1500 Model) at the heating rate of $10^\circ\text{C}/\text{min}$ under ambient atmosphere. The microstructure of the powder was observed using JEOL (JSM-840 A) scanning electron microscope.

2.3 Electrochemical characteristics

$\text{LiMg}_y\text{Mn}_{2-y}\text{O}_4$ powders were electrochemically characterized by fabricating 2016 coin cells which consisted of lithium anode, $\text{LiMg}_y\text{Mn}_{2-y}\text{O}_4$ powder cathode, polypropylene separator and a solution of 1 M Li PF $_6$ in 1 : 1 (v/v) ratio of EC and DEC electrolyte. The cathode was made of a mixture containing $\text{LiMg}_y\text{Mn}_{2-y}\text{O}_4$ powder, acetylene black and polyvinylidene fluoride (PVdF) binder in N-methyl-2-pyrrolidone (NMP) in the 80 : 10 : 10 weight ratio. This mixture was spread over an expanded microgrid and was then pressed at a pressure of 5 tons/cm 2 and dried at 120°C for 5 h in an oven. The cells were assembled in an argon filled dry box. The charge and discharge

cycling was performed galvanostatically at the current density of 0.2 mA/cm 2 within voltages of 3.2–4.5 V.

3. Results and discussion

The optimum temperature of phase formation and/or crystallization of the $\text{LiMg}_{0.20}\text{Mn}_{1.80}\text{O}_4$ precursor sample is 490.17°C which is confirmed by thermal analysis as shown in figure 1. This result displays two discrete weight loss regions occurring at 381.5°C and 490.2°C . An endothermic peak is observed at about 381.49° accompanied by a noticeable weight loss of 2.5%. With continuous heating, the mass loss increases, owing to the combustion nature of citric acid together with nitrate precursor complexes and resulting in second exotherm whose onset begins at 490.2°C with an end at 534.5°C accompanied by huge mass loss of 70.4%. This indicates that the compound begins to decompose at lower temperatures and the exothermic combustion of citric acid supplying adequate heat energy for initiating the crystallization of $\text{LiMg}_y\text{Mn}_{2-y}\text{O}_4$ powder. There are two distinguishable exothermic transformations deduced from the DTA data. The exotherm occurring at 490.2°C indicates phase formation and/or crystallization of the cubic spinel, $\text{LiMg}_x\text{Mn}_{2-x}\text{O}_4$.

Figure 2 shows X-ray diffraction patterns of a series of powders with different x in $\text{LiMg}_y\text{Mn}_{2-y}\text{O}_4$ materials calcined at 550°C for 5 h in air. All these samples were identified as a single phase cubic spinel with a space group, $Fd\bar{3}m$. The lattice constant values of $\text{LiMg}_y\text{Mn}_{2-y}\text{O}_4$ samples were presented in table 1. As compared with LiMn_2O_4 , the lattice parameters of $\text{LiMg}_y\text{Mn}_{2-y}\text{O}_4$ slightly decreased with increase in substitution of Mg^{2+} content (Liu *et al* 1996; Idemoto *et al* 1999) and hence the Bragg planes (440) and (531) were slightly shifted towards lower 2θ angle. Figure 3 represents the variation of the cubic lattice parameters of $\text{LiMg}_y\text{Mn}_{2-y}\text{O}_4$ as a function of the Mg content. It is obvious that a slight decrease in lattice parameter was observed due to the partial replacement of Mn by Mg^{2+} . This increases the average Mn

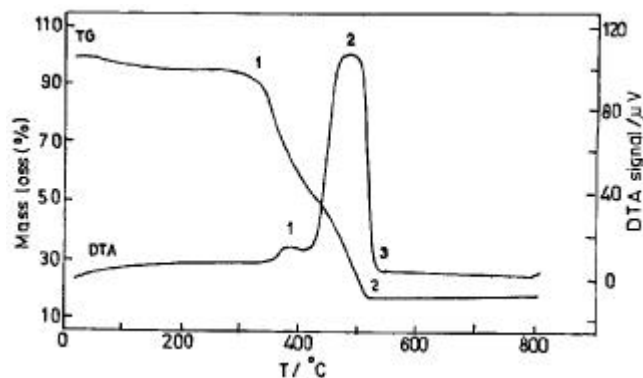


Figure 1. TG and DTA scans of the precursor sample, $\text{LiMg}_{0.20}\text{Mn}_{1.80}\text{O}_4$.

valency from Mn^{3+} to Mn^{4+} . Also the Mg^{2+} replaces Mn^{3+} in the 16 d octahedral site and hence the strong Bragg plane (220) was not observed at $2\theta = 30^\circ$, which is extremely sensitive to the occupancy of the 8a tetrahedral site (Julien *et al* 2001).

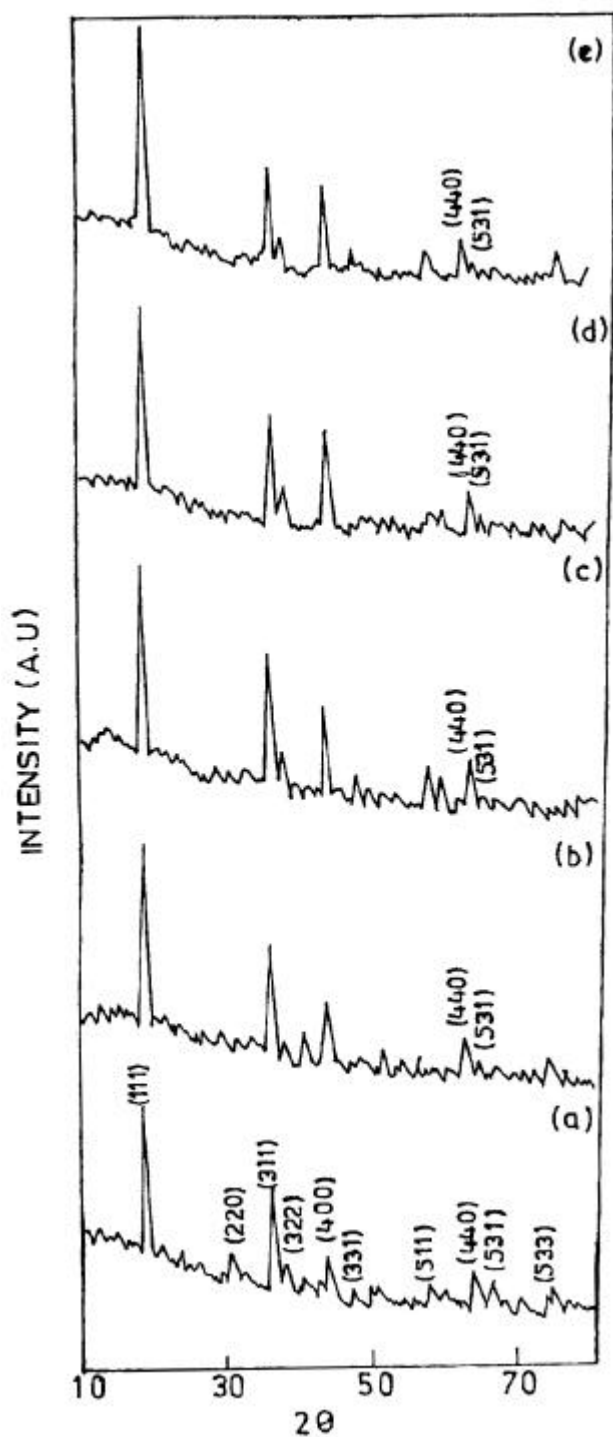


Figure 2. X-ray diffraction patterns for cubic spinel, $\text{LiMg}_y\text{Mn}_{2-y}\text{O}_4$, where (a) $y = 0.0$, (b) $y = 0.05$, (c) $y = 0.10$, (d) $y = 0.15$ and (e) $y = 0.20$ obtained by modified Pechini process.

The 4 V discharge capacities of the cathodes of various compositions obtained in the first cycle (figure 4) along with the theoretical values are shown in table 2. The initial discharge capacities of $\text{Li}/\text{LiMn}_2\text{O}_4$ ($y = 0$) is 137 mAh/g. The initial discharge capacities of $\text{Li}/\text{LiMg}_y\text{Mn}_{2-y}\text{O}_4$ from $y = 0$ to 0.25 are 132 mAh/g, 118 mAh/g, 100 mAh/g and 90 mAh/g, respectively. Since deintercalation of Li^+ from the spinel structure must be electrically compensated by oxidation of Mn^{3+} to Mn^{4+} . This suggests that even for substituted spinel phases, only the amount of Mn^{3+} contributes to the discharge capacity. So the initial capacity of $\text{LiMg}_y\text{Mn}_{2-y}\text{O}_4$ ($0 \leq y \leq 0.25$) is limited by the initial amount of Mn^{3+} in the 16 d sites. The discharge capacity versus cycle number of $\text{Li}/\text{LiMg}_y\text{Mn}_{2-y}\text{O}_4$ with $y = 0$ to 0.25 is shown in figure 5. The capacity loss observed for undoped LiMn_2O_4 is about 25% after 25 cycles, whereas that for $\text{Li}/\text{LiMg}_y\text{Mn}_{2-y}\text{O}_4$ from $y = 0.05$ to 0.25 are 12%, 2.33%, 7% and 9.5%, respectively. This can be achieved by the substitution of Mg^{2+} into the Mn site accompanied

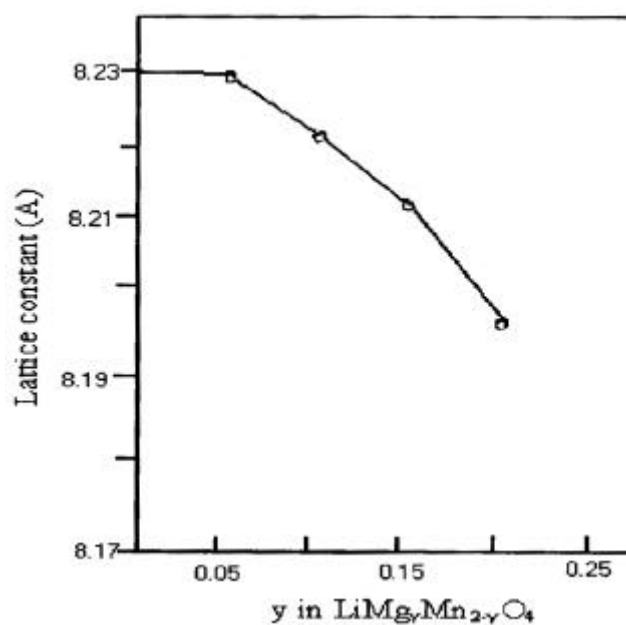


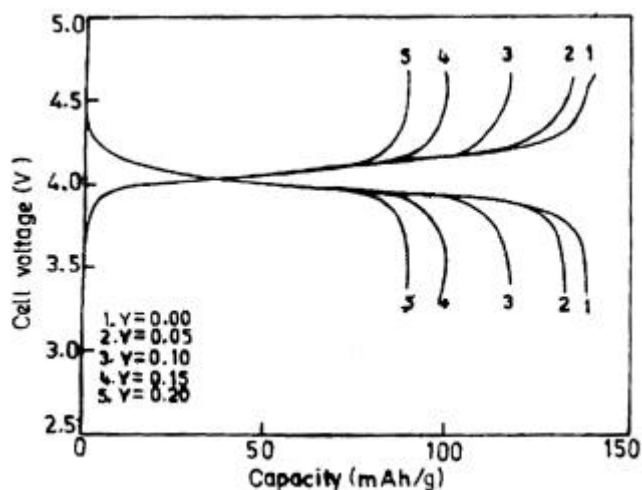
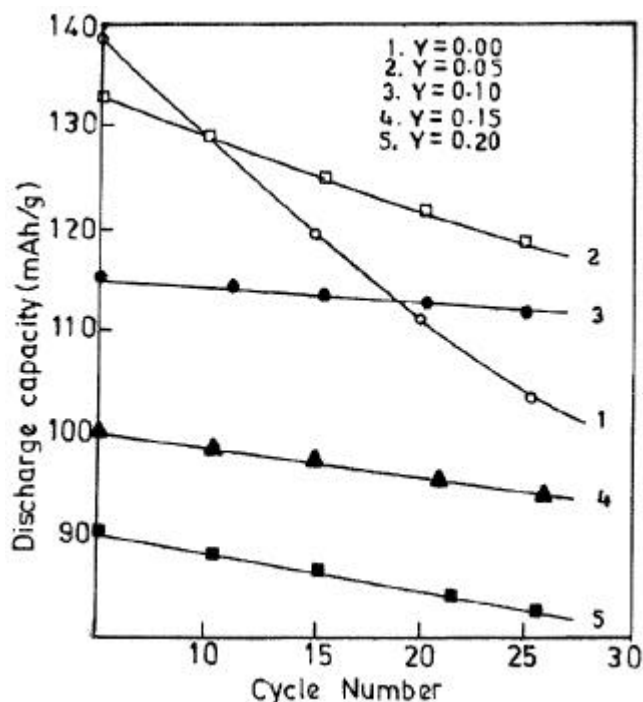
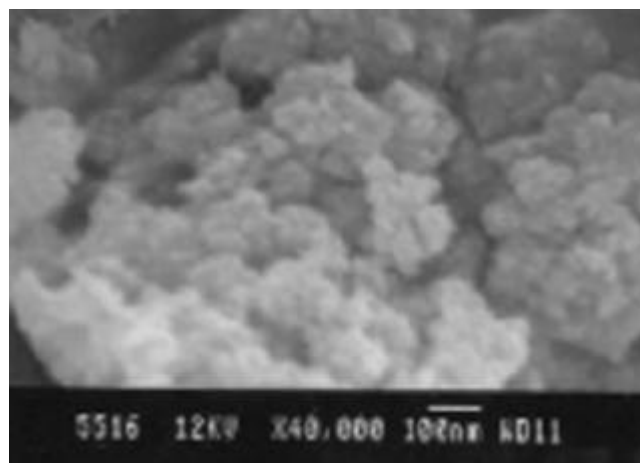
Figure 3. Variation of lattice constant of $\text{LiMg}_y\text{Mn}_{2-y}\text{O}_4$ as a function of Mg content.

Table 1. Comparison between the standard and experimentally observed lattice constant values of cubic spinel, $\text{LiMg}_y\text{Mn}_{2-y}\text{O}_4$.

Compound	Standard lattice constant value (Å)	Experimentally observed lattice constant value (Å)
LiMn_2O_4	8.2358	8.2293
$\text{LiMg}_{0.05}\text{Mn}_{1.95}\text{O}_4$	8.2356	8.2287
$\text{LiMg}_{0.1}\text{Mn}_{1.9}\text{O}_4$	8.2338	8.2205
$\text{LiMg}_{0.15}\text{Mn}_{1.85}\text{O}_4$	8.2191	8.2123
$\text{LiMg}_{0.2}\text{Mn}_{1.8}\text{O}_4$	8.2154	8.1976

Table 2. 4 V capacities of various compositions (mAh/g).

Formula	Practical capacity	Theoretical capacity
$\text{LiMn}_2\text{O}_4 [\text{Li}]_{8a} [\text{Mn}^{3+}\text{Mn}^{4+}]_{16d} [\text{O}_4]_{32e}$	137	148.2
$\text{LiMg}_{0.05}\text{Mn}_{1.95}\text{O}_4 [\text{Li}]_{8a} [\text{Mg}^{2+}_{0.05}\text{Mn}^{3+}_{0.9}\text{Mn}^{4+}_{1.05}]_{16d} [\text{O}_4]_{32e}$	132	134.5
$\text{LiMg}_{0.1}\text{Mn}_{1.9}\text{O}_4 [\text{Li}]_{8a} [\text{Mg}^{2+}_{0.10}\text{Mn}^{3+}_{0.8}\text{Mn}^{4+}_{1.10}]_{16d} [\text{O}_4]_{32e}$	118	120.61
$\text{LiMg}_{0.15}\text{Mn}_{1.85}\text{O}_4 [\text{Li}]_{8a} [\text{Mg}^{2+}_{0.15}\text{Mn}^{3+}_{0.7}\text{Mn}^{4+}_{1.15}]_{16d} [\text{O}_4]_{32e}$	100	106.45
$\text{LiMg}_{0.2}\text{Mn}_{1.8}\text{O}_4 [\text{Li}]_{8a} [\text{Mg}^{2+}_{0.20}\text{Mn}^{3+}_{0.6}\text{Mn}^{4+}_{1.20}]_{16d} [\text{O}_4]_{32e}$	90	92.046

**Figure 4.** Electrochemical features of Li/LiMg_yMn_{2-y}O₄ cells with $y = 0.0, 0.05, 0.10, 0.15, 0.20$ during first charge-discharge cycle in the voltage range of 3.2 and 4.5 V at a current density of 0.2 mA/cm².**Figure 5.** Relationship between the discharge capacity and cycle number of Li/LiMg_yMn_{2-y}O₄ cells in the voltage range of 3.2–4.5 V at a current density of 0.2 mA/cm².**Figure 6.** Scanning electron micrograph of the cubic spinel, LiMg_{0.10}Mn_{1.90}O₄, obtained by modified Pechini process.

by the oxidation of Mn³⁺ into Mn⁴⁺ resulting in an increase in the average valency of Mn which suppresses the John–Teller distortion. Li *et al* (1996) also reported that the doped materials enhance the stability of the octahedral sites in the spinel skeleton structure. Hence, the electrochemical stability of LiMn₂O₄ is less than that of the Mg substituted LiMn₂O₄. These results were in good agreement with the reported results (Jeong *et al* 2001). Among the various compositions, LiMg_{0.10}Mn_{1.90}O₄ shows better reversibility, because the suppression of John–Teller distortion is high in 0.10 substitution than 0.05 substitution. Moreover, electrochemically inactive Mn⁴⁺ species is low in 0.10 substitution than in 0.15, 0.20 and 0.25 substitutions. Figure 6 shows the scanning electron microscope (SEM) pattern of LiMg_{0.10}Mn_{1.90}O₄ powder calcined at 550°C for 5 h in air. The photograph confirms the formation of spherical grains of sub-micron nature of lithium magnesium manganate with an average size of < 50 nm accompanied by controlled grain growth.

4. Conclusions

The following conclusions were drawn from the present study:

(I) The modified Pechini process is found to be an easy method for the synthesis of cubic spinel, LiMg_yMn_{2-y}O₄ powders, at moderate temperature.

(II) X-ray diffraction analysis confirms the phase purity and the structure of the synthesized products.

(III) Thermal analysis indicates the exact phase formation and/or crystallization temperature of the $\text{LiMg}_{0.20}\text{Mn}_{1.80}\text{O}_4$ sample. It is found that the product undergoes complete crystallization at 535°C .

(IV) The SEM analysis confirms the formation of spherical grains of < 50 nm accompanied by controlled grain growth of the powder.

(V) The charge–discharge behaviour of the synthesized $\text{LiMg}_{0.10}\text{Mn}_{1.90}\text{O}_4$ sample shows the initial discharge capacity of 118 mAh/g and its capacity loss at even 25th cycle is only 2.33%.

Thus the modified Pechini process used in this investigation is found to be a very useful process for synthesizing Mg-doped LiMn_2O_4 spinel at moderate temperature which has good cyclability. Hence, the compound could be used as an effective cathode material for high voltage rechargeable lithium batteries.

Acknowledgements

The authors gratefully acknowledge DST, New Delhi, for financial support.

References

- Bach S, Henry M, Baffier N and Livaje J 1990 *J. Solid State Chem.* **88** 325
- Barboux P, Tarascon J M and Shokoohi F K 1991 *J. Solid State Chem.* **94** 185
- Gummow R J, Dekock A and Thackeray M M 1994 *Solid State Ionics* **69** 59
- Guyomard D and Tarason J M 1994 *Solid State Ionics* **69** 222
- Hwang B J, Santhanam R and Liu D G 2001 *J. Power Sources* **101** 86
- Idemoto Y, Koura N and Udagawa Y 1999 *J. Electrochem. Soc. Jap.* **67** 235
- Jain S R, Adiga K C and Pai V R 1981 *Comb. Flame* **40** 71
- Jeong I S, Kim J and Gu H B 2001 *J. Power Sources* **102** 55
- Julien C, Ziolkiewicz S, Lemal M and Massot M 2001 *J. Mater. Chem.* **11** 1837
- Kovacheva D, Hristo, Petrov K and Sankar M 2002 *J. Mater. Chem.* **12** 1184
- Lee J H, Jin K, Hong J K, Jang D H, Sun Y-K and Seung M O 2004 *J. Power Sources* **89** 7
- Li G, Ikuta H, Uchida M and Wakihara M 1996 *J. Electrochem. Soc.* **143** 178
- Liu D G, Farrington G C, Chaput F and Dunn B 1996 *J. Electrochem. Soc.* **143** 876, 3590
- Morita M, Nakagawa T, Yamada O, Yoshimoto N and Ishikawa M 2001 *J. Power Sources* **97** 354
- Myung S T, Chung H T, Komaba S, Kumagai N and Gu H B 2000 *J. Power Sources* **90** 103
- Ozhuku T, Kitagawa M and Hirai T 1990 *J. Electrochem. Soc.* **137** 760
- Shaju K M, Subba Rao G V and Chowdari B V R 2002 *J. Electrochim. Acta* **48** 145
- U.S. Pat. 1967 3,330,697
- Yamada A 1996 *J. Solid State Chem.* **122** 160